A Novel Equalizer for 112 Gb/s CAP-Based Data Transmission over 150 m MMF links

X. Dong, N. Bamiedakis, D. G. Cunningham, R.V. Penty and I. H. White

***Abstract*—In this paper a novel feedforward and decision feedback equalizer is proposed for the first time for use in short-reach high-speed communication links based on carrierless amplitude and phase (CAP) modulation. The proposed new equalizer mitigates crosstalk between the in-phase (I-) and quadrature (Q-) channels resulting from the non-linear phase response of the link enabling significant improvement in the link performance when operating at high data rates. The structure of this novel equalizer is introduced, its operation is described, and simulation and experimental studies on short-reach high-speed MMF links using 850 nm multimode VCSELs are presented. Data transmission tests are carried out over 150 m of OM4 MMF at 112 Gb/s using CAP modulation and the proposed CAP equalizer, and a bit-error-rate (BER) within the hard-decision forward error-correction (HD-FEC) threshold of 3.8×10^{-3} is achieved. The link is also tested when a conventional equalizer is used instead of the CAP equalizer and when adaptive discrete multitone (DMT) modulation is applied. The performance of the link is compared for these different transmission schemes and it is shown that the use of the novel equalizer and CAP modulation outperforms the other two schemes. The proposed equalizer can be implemented with low additional complexity, providing a potential cost-effective solution enabling > 100 Gb/s single-lane data transmission in short-reach MMF-based links.**

***Index Terms*—Carrierless amplitude and phase (CAP) modulation, equalizers, fiber optics communication, short-range communications, vertical-cavity surface-emitting lasers (VCSELs).**

I. Introduction

With the ever-increasing demand for data traffic inside data centres, current research is focused on improving the achievable data rates in short-range optical links. 400 Gb/s optical links are being targeted as the next generation of short-reach communication links inside data centres [1]. This target can be achieved with different configurations such as by deploying 16 lanes each operating at 25 Gb/s or 8 lanes at 50 Gb/s. However, such multi-lane configurations impose stringent requirements in terms of the power consumption, footprint and number of active and passive components in the link [2, 3]. A single-lane 100 Gb/s data link can provide some important advantages such as smaller footprint and lower power consumption, facilitating the implementation of next generation 400 Gb/s optical links.

The majority of short-reach optical links inside data centres consists of multimode fibre (MMF) links based on 850 nm multimode (MM) vertical cavity surface-emitting lasers (VCSELs). MM VCSELs are attractive components for use in such links as they exhibit relatively high output powers (> 1 mW) and large bandwidths (> 20 GHz) [4], are power efficient due to their low threshold current (~ 1 mA), are low cost, can be formed in large arrays and are readily interfaced with multimode ribbon fibres. Additionally, they are relatively insensitive to temperature effects, hence don't require temperature control and have a large enough output spectrum to minimize modal noise effects [5]. Record-high data rates of 70 Gb/s and 64 Gb/s have been achieved using non-return-to-zero (NRZ) modulation [6, 7]. Similarly, there has been increasing interest in recent years on single mode (SM) VCSELs operating at longer wavelengths (~ 1.31 μm and 1.55 μm) as they can enable low-cost optical links over SMF and therefore achieve longer optical links (> 1 km) in data centre environments [8, 9].

However, achieving data rates ≥100 Gb/s over VCSEL-based MMF links using a single source is challenging due to the limited bandwidth of the active devices and of the multimode fibre itself. Therefore, recent research has concentrated on spectrally-efficient, advanced modulation formats, such as pulse amplitude modulation (PAM) [10], carrier-less amplitude and phase (CAP) modulation [11] and discrete multitone (DMT) modulation [12]. Additionally, equalization is typically used at the receiver (Rx) in high-speed links in order to mitigate the inter-symbol interference (ISI) caused by the limited bandwidth of the active components and fibre allowing successful recovery of the transmitted symbols. The equalizers typically employed comprise feed-forward (FFE) and decision feedback (DFE) equalizers [20].

Numerous high-speed VCSEL-based links achieving >100 Gb/s transmission over MMF have been reported in recent years by deploying multi-carrier and multi-level modulation schemes with equalization. For example, a multiband-CAP modulation has been employed to achieve 100 Gb/s data rate over 10 m OM4 MMF [11]. 150 Gb/s and 112 Gb/s data transmission have been reported over 100 m of OM4 MMF fibre using duobinary PAM-4 [10] and DMT [13] respectively.

Manuscript received June xx, 2019; revised August xx, 2019; accepted September xx, 2019. Date of publication February xx 2019; date of current version November xx, 2018.
The authors would like to acknowledge the UK EPSRC for supporting this work via the Terabit Bidirectional Multi-user Optical Wireless System project (TOWS) (EP/S016570/1).
Additional data related to this publication is available at the data repository https://doi.org/10.17863/CAM.40707.
X. Dong, N. Bamiedakis, D.G. Cunningham, R. V. Penty and I. H. White are with the Centre for Photonic Systems, Electrical Engineering Division, Department of Engineering, University of Cambridge, Cambridge CB3 0FA, U.K. (e-mail: xd232@cam.ac.uk).
Digital Object Identifier 10.1109/xxxx

In [12], pre-distortion and DMT modulation have been employed to demonstrate the transmission of 122 Gb/s over 10 m of OM4 MMF with a bit-error-rate (BER) within the soft-decision forward error correction (SD-FEC) threshold.

CAP modulation is a particularly interesting modulation scheme as it utilizes two orthogonal passband filters (in-phase and quadrature) to encode the baseband signal and is easier to implement than quadrature amplitude modulation (QAM) schemes [14]. Multi-carrier CAP schemes (M-CAP) have also been proposed and demonstrated in high-speed optical links [11]. However, single-carrier CAP has lower system complexity as it requires a smaller number of filters than M-CAP. Furthermore, it offers important advantages over the equivalent PAM scheme, namely removing baseline wander whilst requiring similar bandwidth with very small additional implementation complexity. However, if the phase response of the link is non-linear, CAP modulation suffers from crosstalk between the in-phase (I-) and quadrature phase (Q-) channels. We propose a novel equalizer for use with CAP modulation, named the CAP equalizer. The new equalizer mitigates the effect of the non-linear phase response in the link, and therefore significantly improves the link performance over conventional FFE and DFE equalizers. Although here the proposed CAP equalizer and therefore, the channel crosstalk mitigation, are implemented at the receiver side of the link, a similar approach can be applied at the transmitter by using two short FFE's between the I and Q channels to pre-distort the transmitted signals. This alternative implementation is currently under study and we hope to report on this in the near future.

In the sections that follow, the structure and operation of the proposed equalizer are described (section II.A), simulation studies on the achievable performance are presented (section II.B) and experimental results on an 850 nm VCSEL-based 150 m OM4 MMF link operating at 112 Gb/s are reported (section III). The performance of the link is compared via simulation and experiments with that obtained when a conventional FFE and DFE equalizer of the same length is employed and when DMT and PAM modulation is applied in the link. It is shown that the conventional equalizer fails at this data rate and that the use of the CAP equalizer provides a 2 dB improvement in the receiver sensitivity for 112 Gb/s transmission compared with the DMT scheme. Although the results shown here are for a MM VCSEL and OM4 MMF link, the same type of equalizer can be applied in SMF links.

II. Theory and Simulation Study

A. CAP Modulation

CAP modulation is a passband modulation scheme which was first proposed in the mid 70s by Falconer et al. at Bell Labs [11]. CAP is similar in principle to QAM but with a simpler implementation as it relies on the use of digital filters to separate the two orthogonal I- and Q- channels. As a result, it offers low power consumption and footprint while achieving the same spectral efficiency as QAM. In the 1990s, it was widely used in digital subscriber lines [15]. The typical CAP-based transmission system is shown in Fig.1.

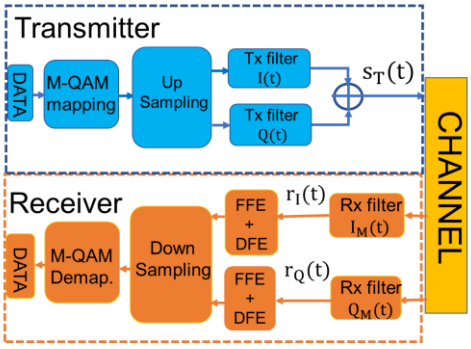

Fig.1. Typical CAP-based transmission system.

The input data is divided into two parallel data streams (QAM-mapping), which are then up-sampled and encoded by the in-phase (I-) and quadrature (Q-) channel pulse shaping filters. The two channels are combined and the resulting composite signal modulates the optical transmitter. For example, CAP-16 is generated by the addition of two PAM-4 streams encoded with the I- and Q- channel filters, respectively. The impulse response of the I- and Q- channel filters is formed by the product of a square root raised cosine (SRRC) filter and a cosine (I-channel) or sine (Q-channel) function. The mathematical expression that describes the transmitted CAP signal $s_T(t)$ is given in (1).

$$s_T(t) = D_I(t) \otimes I(t) + D_Q(t) \otimes Q(t) \quad (1)$$

where $I(t)$ and $Q(t)$ are the pre-defined pulse shaping functions of the I- and Q-channel transmit (Tx) filters and "⊗" is the convolution operator. $D_I(t)$ and $D_Q(t)$ represent the I- and Q-channel symbol streams.

At the receiver end (Rx), the time domain demodulated signal $r_I(t)$ and $r_Q(t)$ can be expressed as (2) and (3).

$$r_I(t) = s_R(t) \otimes I_M(t) \quad (2)$$

$$r_Q(t) = s_R(t) \otimes Q_M(t) \quad (3)$$

The condition for separating the I- and Q- channel symbols at the receiver side (Rx) is stated in (4) and (5).

$$\angle I_M(\omega) \equiv \angle Q(\omega) + \frac{\pi}{2} \quad (4)$$

$$\angle Q_M(\omega) \equiv \angle I(\omega) + \frac{\pi}{2} \quad (5)$$

where $\angle I(\omega)$ and $\angle Q(\omega)$ are the phase spectrum of I- and Q- Tx filters, $\angle I_M(\omega)$ and $\angle Q_M(\omega)$ are the phase spectrum of I- and Q- Rx matched filters. The phase difference of $\frac{\pi}{2}$ which appears in (4) and (5) indicates the orthogonality of I- and Q-channels, and guarantees the independent demodulation of the I- and Q- channels without any crosstalk.

Assuming that the optical link has an impulse response $h(t)$, the received signal $s_R(t)$ is given by the expression (6).

$$s_R(t) = s_T(t) \otimes h(t) \quad (6)$$

Combining (1) with (6), the $s_R(t)$ can be expressed as :

$$s_R(t) = D_I(t) \otimes \hat{I}(t) + D_Q(t) \otimes \hat{Q}(t) \quad (7)$$

where $\hat{I}(t) = I(t) \otimes h(t)$ and $\hat{Q}(t) = Q(t) \otimes h(t)$. The functions $\hat{I}(t)$ and $\hat{Q}(t)$ describe the combined response of the transmit I- and Q-filters and the optical link. If the link has linear phase response $\angle H(\omega) = k\omega$, the phase spectrum of the combined response of the transmit filters and optical link

$\angle\hat{I}(\omega)$ and $\angle\hat{Q}(\omega)$ become $\angle\hat{I}(\omega)+k\omega$ and $\angle\hat{Q}(\omega)+k\omega$ respectively. This additional linear phase response can be mitigated by time-shifting the received signal by *k*: the time-domain received signal is $s_R(t-k)$ and its phase spectrum becomes $\angle S_R(\omega)-k\omega$. As a result, the phase spectrum can be corrected by (-ωk), which will shift back $\angle\hat{I}(\omega)$ and $\angle\hat{Q}(\omega)$ to $\angle I(\omega)$ and $\angle Q(\omega)$. Therefore, a linear link phase response does not introduce any signal transmission impairment.

However, if the link has a non-linear phase response σ(ω), the phase spectrum of the combined response of the transmit filter and optical link becomes:

$$\angle\hat{I}(\omega) \equiv \angle I(\omega)+\angle\sigma(\omega) \quad (8)$$

$$\angle\hat{Q}(\omega) \equiv \angle Q(\omega)+\angle\sigma(\omega) \quad (9)$$

Now, in order to maintain the signal orthogonality and be able to separate the two channels perfectly at the receiver, the following equations for the phase response of the matched filters $\angle I_M(\omega)$ and $\angle Q_M(\omega)$ need to be satisfied:

$$\angle I_M(\omega) \equiv \angle Q(\omega)+\angle\sigma(\omega)+\frac{\pi}{2} \quad (10)$$

$$\angle Q_M(\omega) \equiv \angle I(\omega)+\angle\sigma(\omega)+\frac{\pi}{2} \quad (11)$$

However, the matched filter $I_M(t)$ and $Q_M(t)$ are pre-defined, and can only satisfy (4) and (5). Due to the nonlinear phase response term $\angle\sigma(\omega)$, equations (10) and (11) cannot be satisfied. As a result, crosstalk between the two channels is generated. For channels suffering linear distortion it is common to use a combination of FFE and DFE equalizers to recover the transmitted symbols, as shown in Fig. 1. However, these conventional equalizers cannot correct non-linear distortion and so cannot combat the crosstalk due to the non-linearity of the channel. Therefore, a novel equalizer, here named the CAP equalizer, is introduced to solve this issue.

B. FFE, DFE and CAP equalizer

Equalization has been widely used in copper cable, radio frequency (RF) and optical links [16, 17] in order to mitigate the ISI induced by the link's bandwidth limitation [18, 19]. Typically, a combination of an FFE and a DFE equalizer is employed in high-speed communication links as such equalizers are more effective in suppressing large amounts of ISI than less complex linear equalizers [20]. In a conventional CAP-based transmission scheme, FFE and DFE (conventional) equalizers are applied separately on each channel to recover the transmitted data [Fig. 2(a)]. However, this equalizer approach cannot mitigate the channel crosstalk described above due to the non-linear phase response of the link. In contrast, the proposed new (CAP) equalizer approach utilizes the signals received on both channels to mitigate the channel crosstalk and recover the transmitted symbols [Fig. 2(b)].

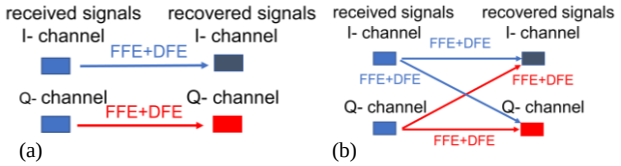

Fig. 2. Structure of (a) a conventional FFE and DFE equalizer and (b) the proposed CAP equalizer.

The operation of an FFE and DFE based equalizer, for the case where the FFE operates on two samples per symbol, is described by the equation:

$$r_k = \sum_{n=0}^{N-1} a_n S_{2k+N-1-n} + \sum_{m=1}^{M} d_m \hat{r}_{k-m} \quad (12)$$

where r_k is the symbol after application of the equalizer (i.e. the recovered symbol) and $\hat{r}_{k-m}$ is the decision on the *k-m* received symbol, N and M are the FFE and DFE tap lengths, a_n and d_m are the FFE and DFE tap coefficients respectively and $S_{2k+N-1-n}$ is the received sample for given *k*, *n* and *N*. Fig. 3(a) shows the structure of an FFE and DFE equalizer with delay lines. For CAP-based transmission, a separate FFE and DFE equalizer is employed on each channel to recover the transmitted symbols. However, as indicated above, the non-linear phase response of the link generates channel crosstalk which prohibits the perfect separation of the two channels at the receiver. This issue cannot be solved by this conventional equalizer as explained in section II.A. As a result, we propose a new FFE and DFE equalizer for CAP-based transmission that aims to mitigate this issue. The detailed structure of this novel equalizer with delay lines is shown in Fig. 3(b). It comprises an FFE and DFE part similar to the conventional, but utilizes the symbols received on both channels to recover the symbols transmitted on each one of them. Eq. (13) provides the expression used to recover the transmitted symbols on the I-channel for this new CAP equalizer:

$$r_k^I = \sum_{n=0}^{N-1} a_n^I S_{2k+N-1-n}^I + \sum_{m=1}^{V} d_m^I \hat{r}_{k-m}^I + \sum_{p=0}^{P-1} a_p^Q S_{2k+P-1-p}^Q + \sum_{l=1}^{L} d_l^Q \hat{r}_{k-l}^Q \quad (13)$$

where r_k^I is the recovered I-channel *k-th* symbol, $\hat{r}_{k-m}^I$ and $\hat{r}_{k-l}^Q$ are the previous *k-m* and *k-l* symbol decisions on I- and Q-channel respectively, a_n^I and d_m^I are the I-channel FFE and DFE tap coefficients, a_p^Q and d_l^Q are the Q-channel FFE and DFE tap coefficients. A similar expression is used to recover the transmitted symbols on the Q-channel but with different coefficient values. It is shown in the simulation studies described below that only a small number of additional taps operating on the other channel are required to achieve significant performance improvement. As a result, the implementation of the proposed CAP equalizer requires small additional complexity in the system implementation.

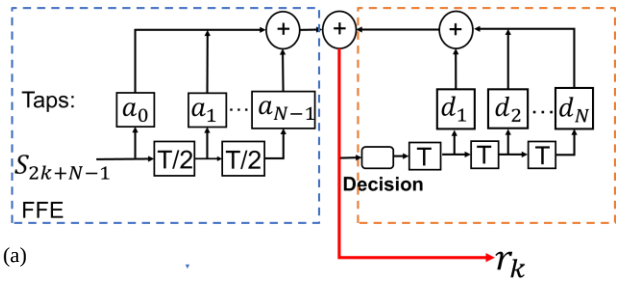

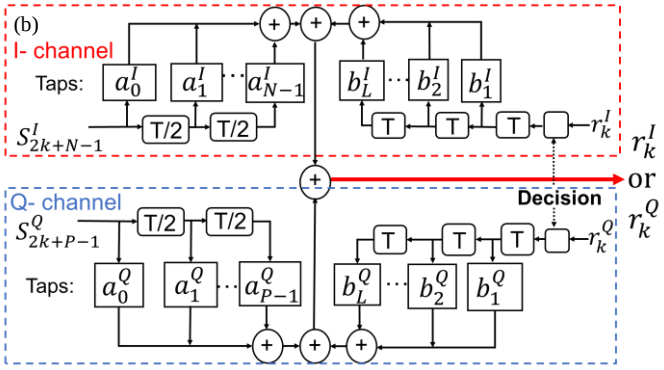

Fig. 3. Detailed structure of (a) the conventional FFE and DFE and (b) the proposed CAP equalizer.

C. Simulation Results

The performance of various links is studied with a link model to simulate the performance of a VCSEL-based OM4 MMF link. The basic components of the link model are shown in Fig. 4 and their main parameters are listed in Table I. The values of the parameters are chosen to match the parameters of the devices used in the data transmission tests reported in section III. The dynamic behaviour of the VCSEL is modelled with a rate equation model which provides the output light waveform for a given modulating signal and bias condition. Its parameters are based on published data on commercially-available directly modulated VCSELs [21]. The fibre and receiver are modelled with a Gaussian and a raised-cosine response, respectively. At the receiver end, equalization is employed to mitigate the ISI of the link. The magnitude and phase of the link's frequency response was calculated for a 100 m long MMF OM4(Fig. 5). The nonlinear phase response of the link can be clearly seen. The performance of the link was calculated when 112 Gb/s CAP-16 modulation (encoded PAM-4 for I-/Q- channel) was applied and when the proposed new CAP and a conventional FFE-DFE equalizer with the same length and tap spacing were used. The tap spacing for the FFE section of both types of equalizer was half of a symbol period (T/2).

TABLE I
LINK SIMULATION PARAMETERS

Component	Response type	-3 dBo / -6 dBe bandwidth	Ref.
VCSEL	Rate equation based	25 GHz	[21]
100 m OM4 MMF	Gaussian	24 GHz	[22]
Receiver	Raised-cosine	30 GHz	[23]

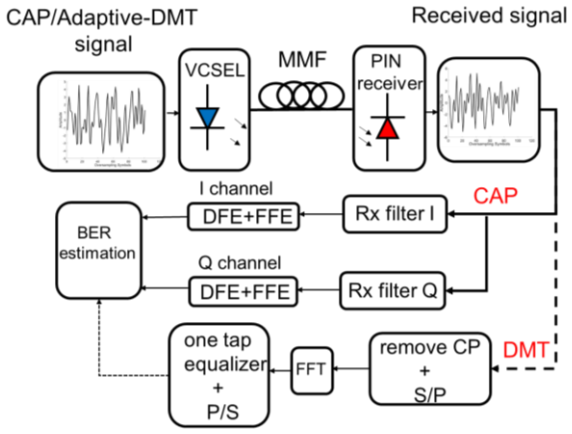

Fig. 4. Block diagram of link model used for CAP and DMT transmission (CP: Cyclic Prefix, S/P: Serial to Parallel, P/S: Parallel to Serial).

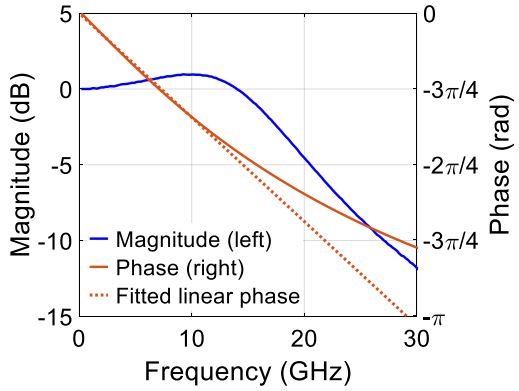

Fig. 5. Simulated magnitude and phase of the frequency response for the VCSEL-based 100 m OM4 MMF link.

For CAP-based transmission, the data pattern used to train the equalizer consisted of a 2^{11}-1 pseudo-random binary sequence (PRBS) which was encoded with a random order into CAP-16 symbols. The training pattern was used to obtain the weight of the equalizer taps using the least mean squares (LMS) algorithm. The data pattern used in the data transmission tests consisted of the same PRBS encoded in the normal order to form the transmitted CAP-16 symbols.

Initially, a representative simulation is performed to demonstrate the channel crosstalk impairment due to the non-linear phase response of the link. A short symbol stream (2^{11}-1 PRBS) is transmitted over the I-channel of the link at both (i) low (9 GBaud, 36 Gb/s) and (ii) high (28 GBaud, 112 Gb/s) symbol rates when the Q-channel is off (no data) and on (transmitting data). For the case of low speed transmission, the spectrum of the transmitted signal mainly falls within the linear range of the phase response of the link (< 10 GHz, Fig. 5) and therefore the orthogonality of the I- and Q-channels is well maintained over the link. As a result, the operation of the Q-channel should not affect the received signal on the I-channel. On the contrary, at the high symbol rate of 28 GBaud, the phase response is non-linear within the signal bandwidth and therefore, the operation of the Q-channel introduces crosstalk distorting the received signal. Fig. 6 shows the demodulated I-channel symbols for the two modes of operation (Q-channel on/off) and two symbol rates before equalization. It can be clearly seen that the operation of the Q-channel only distorts the

received signal on the I-channel at the high symbol rate, indicating the presence of the channel crosstalk due to the non-linear phase response. Similar crosstalk issues also exist for the Q-channel.

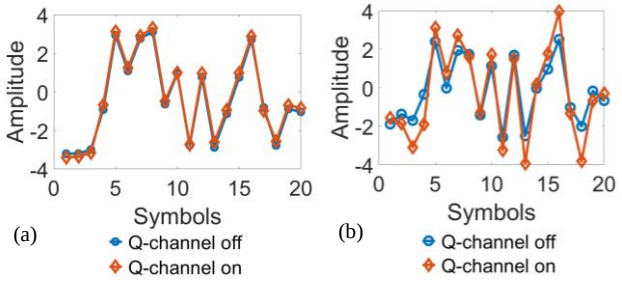

Fig. 6. Demodulated I- channel symbols for the two modes of operation before equalization at two different symbol rates: (a) 9 GBaud(36 Gb/s); (b) 28 GBaud (112 Gb/s).

Additionally, the two types of equalizers (conventional and CAP) are employed to recover the transmitted symbols on the I-channel for the high symbol rate transmission (112 Gb/s) when the Q-channel is transmitting data. Fig. 7 shows the obtained error for the equalizer training for the two equalizers. It can be clearly seen that the conventional equalizer fails to converge, whereas the proposed CAP equalizer yields a converged error within ±0.5.

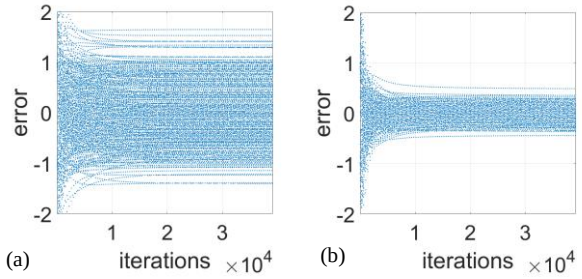

Fig. 7. Obtained errors for the LMS training algorithm at 112 Gb/s over 100 m OM4 fibre: (a) conventional and (b) the CAP equalizer.

Fig. 8 shows the demodulation results obtained with the simulation model for 112 Gb/s CAP-based data transmission over a 100 m OM4 MMF link in the cases where the conventional and CAP equalizers were employed at the receiver: (a) and (c) constellation diagrams, and (b) and (d) eye diagrams for the I-channel after equalization. The conventional equalizer used 25 FFE taps and 25 DFE taps while the CAP equalizer used the same total tap length (20+20 from the I- (main) channel and 5+5 from the Q- (crosstalk) channel). The noise of the received signal has not been included in the diagrams to allow better visualization of the residual ISI in the link and direct comparison of the performance achieved with the two equalizers. Clearly the proposed CAP equalizer yields good constellation and eye diagrams, whereas the conventional equalizer fails to recover the transmitted signal. The CAP equalizer clearly outperforms the conventional equalizer.

In order to assess the additional complexity required for successful signal recovery at this data rate, the error vector magnitude (EVM) was calculated as function of the number of additional taps introduced for each type of equalizer (Fig. 9). The reference performance obtained for 0 additional taps corresponds to a 20-tap FFE and 20-tap DFE conventional equaliser on the I- and Q-channel. The additional taps are equally split between the FFE and DFE (i.e. 2 additional taps correspond to a 21-tap DFE and 21-tap FFE). For the conventional equalizer the additional taps are introduced only in the FFE and DFE of the same channel, while for the CAP equalizer the additional taps are introduced in the FFE and DFE of the other channel. Fig. 9 shows that the conventional equalizer can only achieve an EVM of ~16% and that increasing the number of taps does not provide any significant performance improvements in the link. This is due to the fact that no further suppression of the ISI can be achieved with this type of equalizer. On the contrary, the introduction of equalizer taps on the other channel in the proposed CAP equalizer, results in a significant reduction of the EVM, with ~4% achieved for only 10 additional taps (5 additional DFE and 5 additional FFE taps) from the other channel. The performance improvement for this equalizer also saturates beyond 10 additional taps as the effectiveness of the equalizer cannot be further improved.

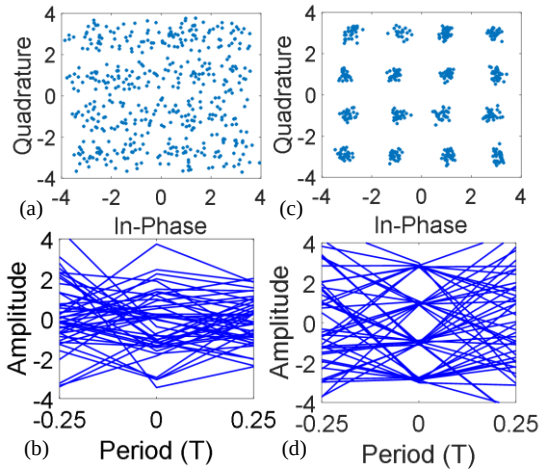

Fig. 8. Simulation results (constellation diagrams and eye diagram for the I-channel after equalisation) for CAP-based 112 Gb/s data transmission over 100 m of OM4 MMF when (a-b) the conventional equalizer and (c-d) the proposed CAP equalizer is employed.

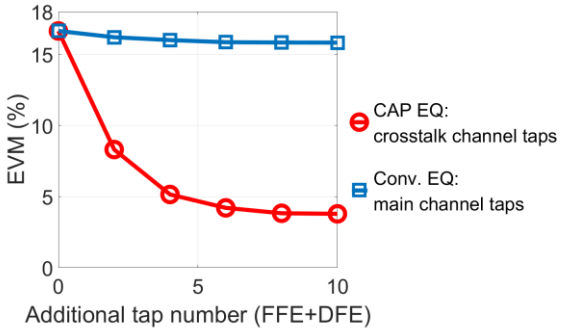

Fig. 9. Calculated EVM as a function of the additional number of taps for both types of equalizer for 112 Gb/s data transmission over 100 m OM4 MMF (Conv: conventional, EQ: equalizer).

At a data rate of 112 Gb/s, the performance of the same link was also simulated when DMT modulation, with adaptive power and bit loading, PAM-4 and PAM-16 modulation were used. This was to allow comparison with the performance obtained with conventional CAP-based transmission and the

newly proposed CAP equalizer. A PRBS pattern of the same length as the one used for the CAP-based transmission is employed to encode the transmitted symbols on each subcarrier. The DMT signal generation contains serial to parallel conversion, adaptive power and bit loading, Hermitian-symmetry operation, inverse fast Fourier transformation (IFFT, length 512), cyclic prefix insertion (15 samples), parallel-serial conversion and clipping (ratio: 5 dB) [12]. The bit and power loading scheme used is shown in Fig. 10(a) and it is based on the estimation of the signal-to-noise ratio (SNR) of the received signal for training sequences consisting of only QAM-4 modulation subcarriers. At the receiver end, a single-tap equalizer was employed for the DMT transmission to recover the transmitted symbols, while for PAM-based transmission a conventional FFE and DFE equalizer with the same length and tap spacing as the CAP equalizer was employed. The BER performance of the CAP, PAM-4 and DMT based links is plotted in Fig. 10(b). The green line indicates the HD-FEC limit. The receiver sensitivity to achieve the BER threshold for HD-FEC limit of 3.8×10^{-3} was found to be -2.4 dBm, -1.2 dBm and -0.7 dBm for the CAP- , PAM-4 and DMT- based links respectively. The use of the proposed CAP equalizer provided a 1.2 dB and 1.7 dB improvement in receiver sensitivity over PAM-4 and DMT respectively. The DMT-based signal transmission suffered from high peak-to-average power ratio (PAPR) and clipping ratio power penalty which resulted in a poorer performance. It was also found that PAM-16 transmission fails at this data rate as the transmitted symbols could not be successfully recovered at the receiver.

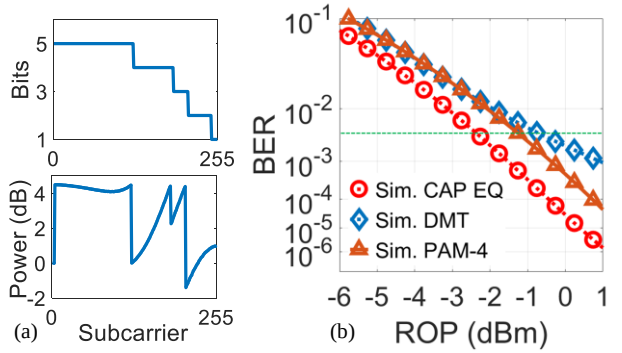

Fig. 10. (a) Adaptive power and bit loading in the DMT modulation scheme. (b) BER plots comparison for the CAP-16 with CAP equalizer, PAM-4 and DMT scheme at 112 Gb/s over 100 m of OM4 MMF (ROP: received optical power).

As a short PRBS length may cause the absence of some amplitude transitions in the transmitted CAP waveforms, the BER performance of the link is also evaluated for a longer PRBS pattern of 2^{15}-1 when the tap coefficients of the CAP equalizer are kept the same as the ones used for the transmission of the 2^{11}-1 data pattern. The obtained BER is shown in Fig. 11 and is compared with that obtained for the shorter pattern. A very similar performance is observed with a small difference of 0.3 dB obtained in the receiver sensitivity required to achieve the BER threshold of 3.8×10^{-3} for HD-FEC due to the use of the longer pattern.

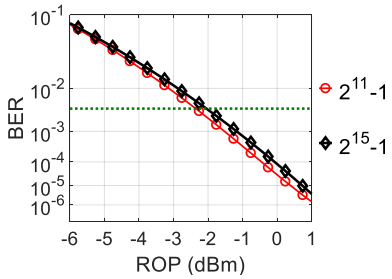

Fig. 11. Simulated BER results for the 112 Gb/s CAP-16 based data transmission over 100 m of OM4 MMF using a 2^{11}- 1 and 2^{15} -1 PRBS pattern (ROP: received optical power).

III. Experiment Results

Data transmission measurements were carried out on an OM4 MMF link using an 850 nm MM VCSEL. The schematic of experimental setup is shown in Fig. 12. At the transmitter end, a 92 GS/s arbitrary waveform generator (AWG, Keysight M8196A) with a 32 GHz analogue bandwidth was used to generate the high-speed modulating signal and a 38 GHz RF amplifier (SHF 806E) was employed to amplify the signal to a peak-to-peak amplitude of 1.5 V. The RF modulating signal was fed to an 850 nm MM VCSEL via a 40 GHz bias tee. The VCSEL had a 3 dB bandwidth of 25 GHz and emitted ~ 7 dBm at the bias current of 12 mA [24, 25]. The emitted light was coupled to a 50 µm MMF patchord via a pair of 16× microscope objectives (numerical aperture of 0.32). A multimode variable optical attenuator (VOA, Agilent N7766A) was employed to adjust the level of the received optical power. Two different lengths of 50 µm OM4 MMF were tested: 100 m and 150 m. The performance for the back-to-back (b2b) link (no OM4 fibre) was also measured to provide a reference for the link performance. At the receiver end, a fibre-coupled 30 GHz PIN photodiode (D30-850M) was used to convert the received optical signal to its electrical counterpart, while a 40 GHz RF amplifier (SHF 807) amplified the electrical signal. The received waveform including 250 periods of the signals was captured with a 70 GHz sampling oscilloscope (Tektronix DPO77002SX). The averaged waveform was calculated and offline processed using Matlab. The offline signal processing included demodulation, equalization and BER estimation as illustrated in Fig. 4. As in the simulation studies, for the CAP-based transmission, the matched filter and equalizer (conventional or CAP equalizer) was applied on each channel to recover the transmitted symbols. The conventional equalizer comprised a 27-tap FFE and a 27-tap DFE for each channel, while each part of the CAP equalizer (FFE and DFE) consisted of 22 taps for the main channel and 5 taps for the other (crosstalk) channel. As a result, both equalizers had the same total length. For the DMT-based transmission, adaptive power and bit loading were employed at the transmitter while at the receiver a single-tap equalizer was used to recover the signal. The estimation of the BER was based on the assumption of Gaussian white noise using the measured root-mean-square noise amplitude for the different levels of average received optical power and considering the noise enhancement introduced by the equalizer.

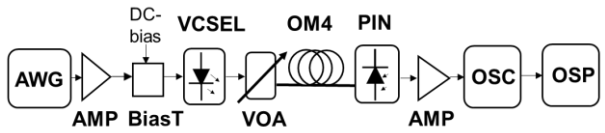

Fig. 12. Experiment setup used in the data transmission tests (AWG: arbitrary waveform generator, AMP: electrical amplifier, VOA: variable optical attenuator, OSC: real-time oscilloscope, OSP: offline signal processing).

Fig. 13 shows the constellation diagram of the averaged received signals for 112 Gb/s CAP-based transmission for the back-to-back (b2b) link and the 100 m and 150 m OM4 MMF links when the conventional and CAP equalizers are employed. It is clear from Fig. 13(a)-(c) that the conventional equalizer enables signal recovery only for the b2b link and fails for both the 100 m and 150 m MMF links. On the other hand, the use of the proposed CAP equalizer yields clear constellation diagrams for all link lengths allowing the successful recovery of the transmitted symbols in all cases, as shown in Fig. 13(d)-(f).

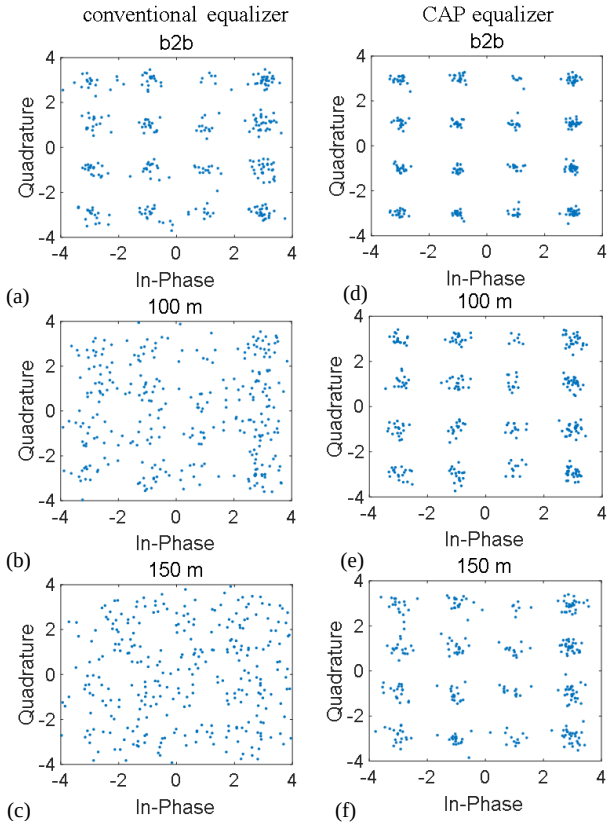

Fig. 13. Constellation diagrams at 112 Gb/s for a received optical power of 0 dBm for the different links and types of employed equalizers: (a)-(c) conventional equalizer and (d)-(f) CAP equalizer.

Fig. 14 shows the error convergence obtained for the two equalizers with the LMS algorithm. It is clear that the conventional equalizer fails to converge to an acceptable error (|error|<1) in contrast to the CAP equalizer. Based on the measured noise, the BER is estimated by adding the appropriate amount of noise, considering the effect of the noise enhancement of the equalizer, to the equalized waveforms. Fig. 15 shows the BER curves obtained for the different links tested. As noted above, the link with the conventional equalizer only works for the b2b case and as a result, only this BER curve is plotted. The use of the equalizer link with the CAP equalizer demonstrates a receiver sensitivity for the HD-FEC BER threshold of -3.8 dBm, -1.9 dBm and 0.5 dBm for the b2b, 100 m and 150 m OM4 MMF link respectively. As in the simulation studies, the BER performance of the 100 m OM4 MMF link when CAP-based transmission and the CAP equalizer are employed are compared with that obtained when DMT modulation is applied. The DMT parameters used in the data transmission tests are the same as the ones used in the simulations. The adaptive power and bit loading scheme applied in the data transmission experiments is shown in Fig. 16(a). The obtained BER curves at 112 Gb/s for the two modulation schemes are shown in Fig. 16(b) as well as the respective plots obtained via the link model. Relatively good agreement between the experimental and simulation results is obtained, with a 0.5 dB difference observed in the obtained receiver sensitivities. The use of CAP modulation in conjunction with the CAP equalizer outperforms the DMT scheme by ~2 dB, achieving a receiver sensitivity of -1.9 dBm for the HD-FEC BER threshold of 3.8×10^{-3}.

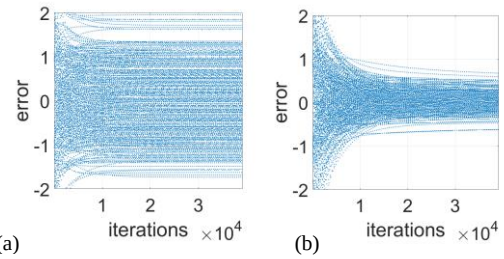

Fig. 14. Training interacted error lines for 112 Gb/s CAP-16 data transmission over 100 m OM4 fibre for (a) the conventional and (b) the CAP equalizer.

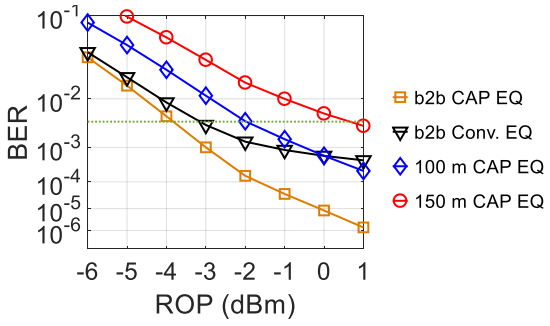

Fig. 15. Experimental results at 112 Gb/s: comparison of BER performance for the CAP equalizer and conventional equalizer for the (b2b), 100 m and 150 m OM4 MMF links (ROP: received optical power).

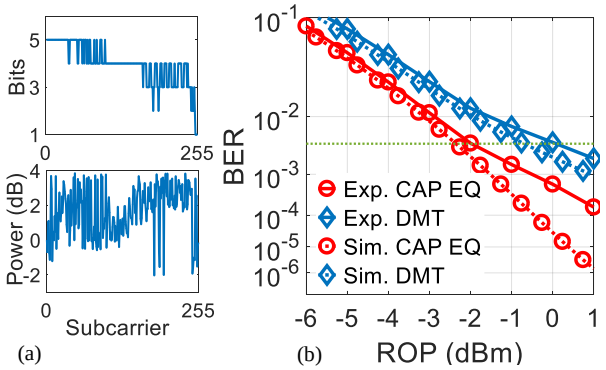

Fig. 16 (a) Bit and power loading used in the DMT scheme and (b) comparison of BER performance obtained at 112 Gb/s over 100 m OM4 MMF with the

CAP equalizer and DMT scheme (Exp.: experimental, Sim.: simulated, ROP: received optical power).

IV. Conclusion

A novel equalizer structure named the CAP equalizer is proposed for use in conjunction with CAP modulation short-reach high-speed optical links. The proposed equalizer uses the data transmitted on both I- and Q- channels of the link in order to recover the transmitted symbol on each one of them to mitigate the impairment due to the non-linear phase response of the link. The significant performance improvement that this equalizer can achieve over a conventional DFE and FFE equalizer of the same length was demonstrated via simulation studies and data transmission tests on short-reach VCSEL-based OM4 MMF links. Both simulation and experiment results demonstrated that the proposed CAP equalizer greatly outperforms the conventional equalizer, and that the combination of CAP modulation and the proposed CAP equalizer provides better BER performance over the use of adaptive DMT and PAM modulation on the same link. The use of the CAP equalizer enabled CAP-based 112 Gb/s data transmission over 100 and 150 m of OM4 MMF with a receiver sensitivity of -1.9 dBm and 0.5 dBm respectively for the HD-FEC BER threshold of 3.8×10^{-3}. The conventional FFE and DFE equalizer failed to support the same data rate over the same links while the use of the DMT modulation yielded poorer receiver sensitivity. The proposed CAP equalizer can be implemented without significant additional complexity over the conventional FFE/DFE equalizer structure.

V. Acknowledgement

The authors would like to acknowledge Keysight for supplying the arbitrary waveform generator for the data transmission tests.

References

[1] I. E. W. Group, "400 gigabit Ethernet call-for-interest consensus," ed: IEEE, 2013.

[2] C.Cole, "Beyond 100G client optics," *IEEE Communications Magazine*, vol. 50, no. 2, pp. 58-66, 2012.

[3] K. Iga and H. Li, *Vertical-cavity surface-emitting laser devices*, Springer, 2003.

[4] D. M. Kuchta, A. V. Rylyakov, C. L. Schow, J. E. Proesel, C. W. Baks, P. Westbergh, J.S. Gustavsson, and A. Larsson, "A 50 Gb/s NRZ modulated 850 nm VCSEL transmitter operating error free to 90 C," *Journal of Lightwave Technology*, vol. 33, no. 4, pp. 802-810, 2014.

[5] P. Pepeljugoski, D. Kuchta, and A. Risteki, "Modal noise BER calulations in 10-Gb/s multimode fiber LAN links," *Photonics Technology Letters*, vol. 17, no. 12, pp. 2586-2588, 2005.

[6] D. Kuchta, A.V. Rylyakov, C.L. Schow, J. Proesel, C. Baks, P. Westbergh, J.S. Gustavsson, and A. Larsson, "64Gb/s Transmission over 57m MMF using an NRZ Modulated 850nm VCSEL," in *Optical Fiber Communication Conference (OFC)*, 2014, paper Th3C.2.

[7] Z. Tan, C. Yang, Y. Zhu, Z. Xu, K. Zou, F. Zhang, and Z. Wang, "A 70 Gbps NRZ optical link based on 850 nm band-limited VCSEL for data-center intra-connects," *Science China Information Sciences*, vol. 61, no. 8, pp. 1-7, 2018.

[8] X. Pang, J. Van, O. Ozolins, R. Lin, A. Udalcovs, L. Zhang, and S. Spiga, "7× 100 Gbps PAM-4 Transmission over 1-km and 10-km Single Mode 7-core Fiber using 1.5-μm SM-VCSEL," in *Optical Fiber Communications Conference (OFC)*, 2018, paper M1I.4.

[9] M. L. Olmedo, J. B. Jensen, Q. Zhong, X. Xu, S. Popov, and L. T. Monroy, "Multiband carrierless amplitude phase modulation for high capacity optical data links," *Journal of Lightwave Technology*, vol. 32, no. 4, pp. 798-804, 2014.

[10] T. Zuo, L. Zhang, J. Zhou, Q. Zhang, E. Zhou, and N. Liu, "Single Lane 150-Gb/s, 100-Gb/s and 70-Gb/s 4-PAM Transmission over 100-m, 300-m and 500-m MMF Using 25-G Class 850nm VCSEL," in *European Conference on Optical Communication (ECOC)*, 2016, pp. 1-3.

[11] R. Puerta, M. Agustin, L. Chorchos, J. Tonski, J. R. Kropp, N. Ledentsov, V. A. Shchukin, N. N. Ledentsov, R. Henker, and I. T. Monroy, "Effective 100 Gb/s IM/DD 850-nm multi-and single-mode VCSEL transmission through OM4 MMF," *Journal of Lightwave Technology*, vol. 35, no. 3, pp. 423-429, 2017.

[12] C. Kottke, C. Caspar, V. Jungnickel, R. Freund, M. Agustin, and N. Ledentsov, "High-speed DMT and VCSEL-based MMF transmission using pre-distortion," *Journal of Lightwave Technology*, vol. 36, no. 2, pp. 168-174, 2018.

[13] B. Wu, X. Zhou, Y. Ma, L. Jun, S. Qiu, Z. Feng, C. Lu, S. Vitaly, K. Joerg, and L. Nikolay, "Single-lane 112Gbps transmission over 300m OM4 multimode fiber based on a single-transverse-mode 850nm VCSEL," in *European Conference on Optical Communication (ECOC)*, 2016, pp. 1-3.

[14] J. D. Ingham, R. V. Penty, I. H. White, and D. G. Cunningham, "40 Gb/s carrierless amplitude and phase modulation for low-cost optical datacommunication links," in *Optical Fiber Communication Conference (OFC)*, 2011, paper OThZ3.

[15] A. F. Shalash and K. K. Parhi, "Multidimensional carrierless AM/PM systems for digital subscriber loops," *IEEE Transactions on Communications*, vol. 47, no. 11, pp. 1655-1667, 1999.

[16] B. Kasper, "Equalization of multimode optical fiber systems," *Bell System Technical Journal*, vol. 61, no. 7, pp. 1367-1388, 1982.

[17] T. S. Rappaport, *Wireless communications: principles and practice*. prentice hall PTR New Jersey, 1996.

[18] L. Geng, J. Wei, R. V. Penty, I.H. White, and D.G. Cunningham, "3 Gbit/s LED-based step index plastic optical fiber link using multilevel pulse amplitude modulation," in *Optical Fiber Communication Conference (OFC)*, 2013, paper OTh4A.1.

[19] J. Wang and J. M. Kahn, "Performance of electrical equalizers in optically amplified OOK and DPSK systems," *Photonics Technology Letters*, vol. 16, no. 5, pp. 1397-1399, 2004.

[20] D. Falconer, S. L. Ariyavisitakul, S. A. Benyamin, and B. Eidson, "Frequency domain equalization for single-carrier broadband wireless systems," *IEEE Communications Magazine*, vol. 40, no. 4, pp. 58-66, 2002.

[21] J. Wang, M. R. Murty, C. Wang, D. Hui, A. L. Harren, H.H. Chang, Z. Feng, T.R. Fanning, A. Sridhara, and S. Taslim, "50Gb/s PAM-4 oxide VCSEL development progress at Broadcom," in *Vertical-Cavity Surface-Emitting Lasers XXI*, 2017, vol. 10122, pp. 1-6.

[22] J.D. Ingham, "Transmitter testing for MMF PMDs," Foxconn Interconnect Technology, San Diego, July, 2016. [Online] Available: http://www.ieee802.org/3/cd/public/July16/ingham_3cd_02a_0716.pdf

[23] http://v-i-systems.com/product/VIS%20Datasheet%20D30-850M.pdf

[24] P. Westbergh, R. Safaisini, E. Haglund, B. Kogel, J.S. Gustavsson, A. Larsson, M. Geen, R. Lawrence, R. Lawrence, "High-speed 850 nm VCSELs with 28 GHz modulation bandwidth operating error-free up to 44 Gbit/s," *Electronics Letters*, vol. 48, no. 18, pp. 1145-1147, 2012.

[25] P. Westbergh, J. S. Gustavsson, B. Kögel, Å. Haglund and A. Larsson, "Impact of photon lifetime on high-speed VCSEL performance," *IEEE Journal of Selected Topics in Quantum Electronics*, vol. 17, pp. 1603-1613, 2011.